


Article

Enhancing the Performance of Evolutionary Algorithm by Differential Evolution for Optimizing Distillation Sequence

Zehua Hu ¹, Peilong Li ² and Yefei Liu ^{1,*} ¹ College of Chemical Engineering, Nanjing Tech University, Nanjing 211816, China; merlinihu0828@gmail.com² Institute of Materials, China Academy of Engineering Physics, Mianyang 621907, China; lipeilong2012@126.com

* Correspondence: yefei.liu@njtech.edu.cn

Abstract: Optimal synthesis of distillation sequence is a complex problem in chemical processes engineering, which involves process structure optimization and operation parameters optimization. The study of the synthesis of distillation sequence is a crucial step toward improving the efficiency of chemical processes and reducing greenhouse gas emissions. This work introduced the concept of binary tree to encode the distillation sequence. The performance of the six evolutionary algorithms was evaluated by solving a 14-component distillation sequence synthesis problem. The best algorithm was used to optimize the operation parameters of a triple-column distillation process. The total annual cost and CO₂ emissions were considered as the metrics to evaluate the performance of triple-column distillation processes. As a result, NSGA-II-DE was found to be the best one of the six tested evolutionary algorithms. Then, NSGA-II-DE was applied to the distillation sequence optimization to find the best operating parameters, which led to a significant reduction in CO₂ emission and total annual costs.

Keywords: distillation process synthesis; distillation sequence; evolutionary algorithm; Aspen Plus

**Citation:** Hu, Z.; Li, P.; Liu, Y.Enhancing the Performance of Evolutionary Algorithm by Differential Evolution for Optimizing Distillation Sequence. *Molecules* **2022**, *27*, 3802. <https://doi.org/10.3390/molecules27123802>

Academic Editor: Susana Valencia

Received: 30 April 2022

Accepted: 9 June 2022

Published: 13 June 2022

Publisher's Note: MDPI stays neutral with regard to jurisdictional claims in published maps and institutional affiliations.



Copyright: © 2022 by the authors. Licensee MDPI, Basel, Switzerland. This article is an open access article distributed under the terms and conditions of the Creative Commons Attribution (CC BY) license (<https://creativecommons.org/licenses/by/4.0/>).

1. Introduction

Design and optimization of distillation sequences become much more essential tasks in process systems engineering, which dramatically influences total annual cost (TAC) and target product purity. The distillation process synthesis was pioneered by Lockhart [1] and systematically analyzed by Siirola et al. [2]. Until now, there have been some popular methods that deal with distillation process synthesis, including the heuristic method, evolutionary method, algorithmic method, and stochastic algorithms. In recent years, many researchers [3,4] focused their attention on distillation process to reduce energy consumption in distillation separation or improve production efficiency, for instance, the coupling of distillation and vapor permeation [5,6] or reactive-vapor permeation-distillation [7]. Although these distillation processes are beneficial to production, design and optimization of distillation sequences are still essential.

Heaven [8] firstly proposed the heuristic method for distillation column optimization. Thompson and King [9] realized automatic calculation of the heuristic method by coding distillation sequences into digits. Freshwater and Henry [10] supplemented inference rules based on Heaven's method. Seader and Westerberg [11] proposed six inference rules to generate the initial separation sequence. The evolutionary method evolved from the heuristic method, which tries out the optimal structure by changing the separation order of key components. Although the heuristic and evolutionary methods have been widely applied in engineering practice, their effectiveness is critically dependent on the completeness of the design engineer's knowledge, and there is no guarantee that the design of a distillation sequence will be optimal. The algorithmic methods introduce mathematical models for nonlinear programming to deal with the problem of distillation

sequences. Nonlinear programming models obtain globally optimal solutions by the gradient descent method. However, due to their non-convex nature, which consistently exhibits in distillation sequence synthesis, the solution often converges to local extrema.

The stochastic algorithms have an attractive advantage over heuristic and evolutionary methods for problems with the modular simulator, where the model for each unit is only in an implicit form (black box model). Firstly, they are based on direct searching methods so that there is no need to have a rigorous model of the problem, which makes it suitable for the processes which are difficult to be modeled. Secondly, the search for the optimal solution is not limited to a single point instead of relying on multiple points contemporaneously, which makes it particularly suitable for handling combinatorial optimization problems with high computational complexity [12].

In recent years, stochastic algorithms have been widely applied for the synchronous optimization of one or more different types of variables. The prevailing stochastic algorithms for the analysis, design, and evaluation of distillation processes have been used directly in the modeling, thus avoiding the sophisticated modeling and handling mixed-integer non-linear programming (MINLP) [13]. Stochastic algorithms can be classified into two main categories according to the dimensionality of the objective function. In the field of single-objective optimization, Floquet et al. [14] applied the simulated annealing (SA) algorithm with a separation-based coding procedure for complex column sequence synthesis. Leboreiro and Acevedo [15] presented a framework for the synthesis and design of complex distillation sequences based on a modified genetic algorithm (GA) coupled with a sequential process simulator. In the last decade, many researchers have evaluated the distillation sequence in multi-dimension to assess the sustainability of the chemical process. Instead, a multi-objective optimization algorithm has been applied. For the multi-objective optimization, Errico et al. [16] proposed an efficient method for the design and optimization of intensified distillation systems by combining the sequential design method and the multi-objective differential evolution. Vázquez-Castillo et al. [17] presented a multi-objective optimization approach that integrates the design and control of multicomponent distillation sequences. Contreras-Zarazúa et al. [18] studied multi-objective optimization involving costs and control properties of intensified schemes to produce diphenyl carbonate. Cabrera-Ruiz et al. [19] introduced a new strategy to consider controllability as an optimization criterion along with the optimal design at a steady state. Alcocer-García et al. [20] used differential evolution with the tabu list in optimizing TAC and the eco-indicator 99. Sun et al. [21] applied an improved multi-objective genetic algorithm to optimize of the triple-column extractive distillation (TCED) process. Zhang et al. [22] suggested a method to solve multi-objective optimization (MOO) in the Fischer–Tropsch reactive distillation synthesis. Zhao et al. [23] combined sequential iterative optimization sequence and a MOO algorithm to optimize equipment costs and CO₂ emissions.

One representative of stochastic algorithms is the so-called evolutionary algorithm, which is widely used for highly non-linear problems. Evolutionary algorithms are a type of stochastic search algorithms which simulate the natural selection and natural evolution of organisms. They mainly include non-dominated sorting genetic algorithm II (NSGA-II) [24], non-dominated sorting genetic algorithm III (NSGA-III) [25], non-dominated sorting genetic algorithm II and III with differential evolution (NSGA-II-DE and NSGA-III-DE) [26], multi-objective evolutionary algorithm based on decomposition (MOEA/D) [27], and multi-objective evolutionary algorithm based on decomposition and differential evolution (MOEA/D-DE) [28]. Although a few studies have been carried out for distillation process synthesis with evolutionary algorithms, nobody has clarified the performances of different evolutionary algorithms, resulting in a lack of guidance for evolutionary algorithms. Furthermore, the role of differential evolution has never been discussed in distillation process synthesis.

In the present study, six evolutionary algorithms were explained and implemented with in-house codes. The performance of the evolutionary algorithms was firstly tested with a 14-component distillation sequence to discern the best one. The effectiveness of

NSGA-II-DE was then examined by optimizing the distillation sequence of a triple-column distillation sequence proposed by Mayevskiy et al. [29]. Finally, some opinions on applying this method to general process synthesis and design issues are provided.

2. Evolutionary Algorithm

2.1. NSGA-II

Deb et al. [24] proposed NSGA-II on the basis of NSGA [30]. In NSGA-II, the evolutionary population is divided into several layers according to the dominance relationship. The dominance of the layers is shown in the schematic diagram of crowding-distance calculation (Figure 1). To obtain an estimate of the density of solutions surrounding a particular solution in the population, NSGA-II calculates the average distance of two points on either side of this point along each of the objectives. In Figure 1, the crowding distance of the i^{th} solution in its front (marked with black squares) is the average side length of the cuboid (shown with a green dashed box). When new populations are generated, the best individuals with relatively low densities are usually retained and participate in the evolution of the next generation.

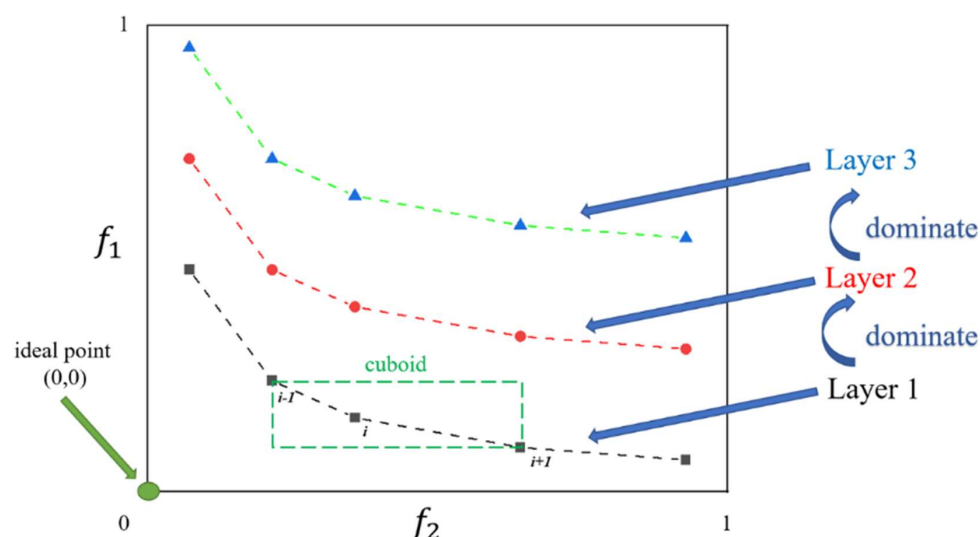


Figure 1. Crowding-distance calculation.

The whole NSGA-II procedure is illustrated in Figure 2. In the N^{st} generation of the parent population, individuals in the population are divided into subpopulations that do not interbreed based on non-dominance sorting, and the individuals satisfying a certain number of subpopulations are selected to enter the next generation of the parent population based on their dominance relationships.

2.2. NSGA-III

NSGA-II handles multi-objective optimization problems very well. However, it is only available for low-dimensional optimization problems (objective dimension less than or equal to 3). As the objective dimension of the optimization problem increases, the number of non-dominated individuals in the population grows exponentially, which makes it challenging to distinguish good and bad individuals in the Pareto dominance. Deb and Jain [25] proposed NSGA-III to solve this problem. The framework of NSGA-III is similar to that of NSGA-II, except that NSGA-III introduces reference lines for the non-dominance ranking of individuals, as shown in Figure 3.

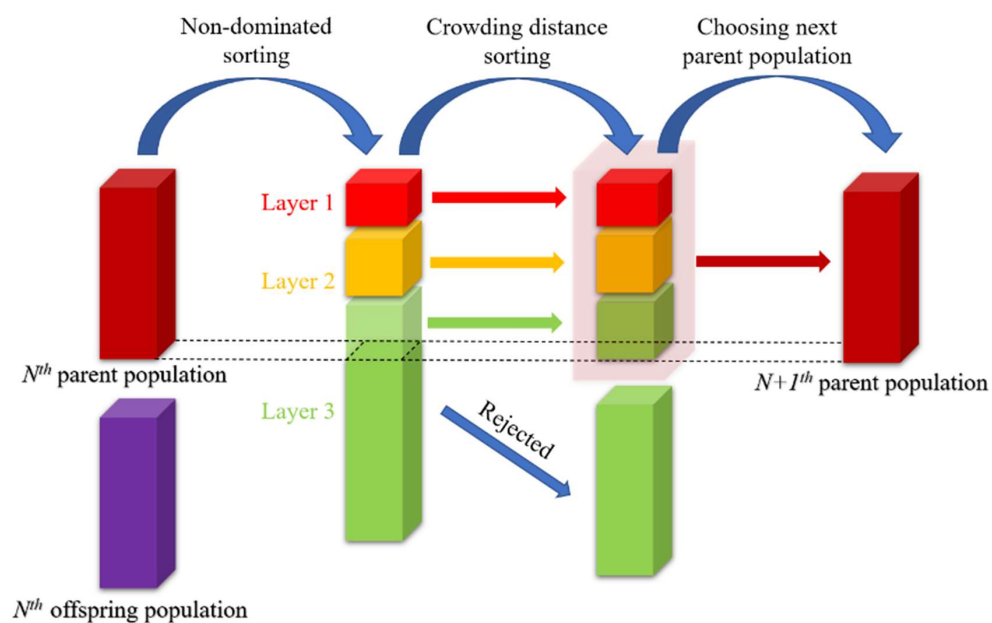


Figure 2. Procedure of NSGA-II.

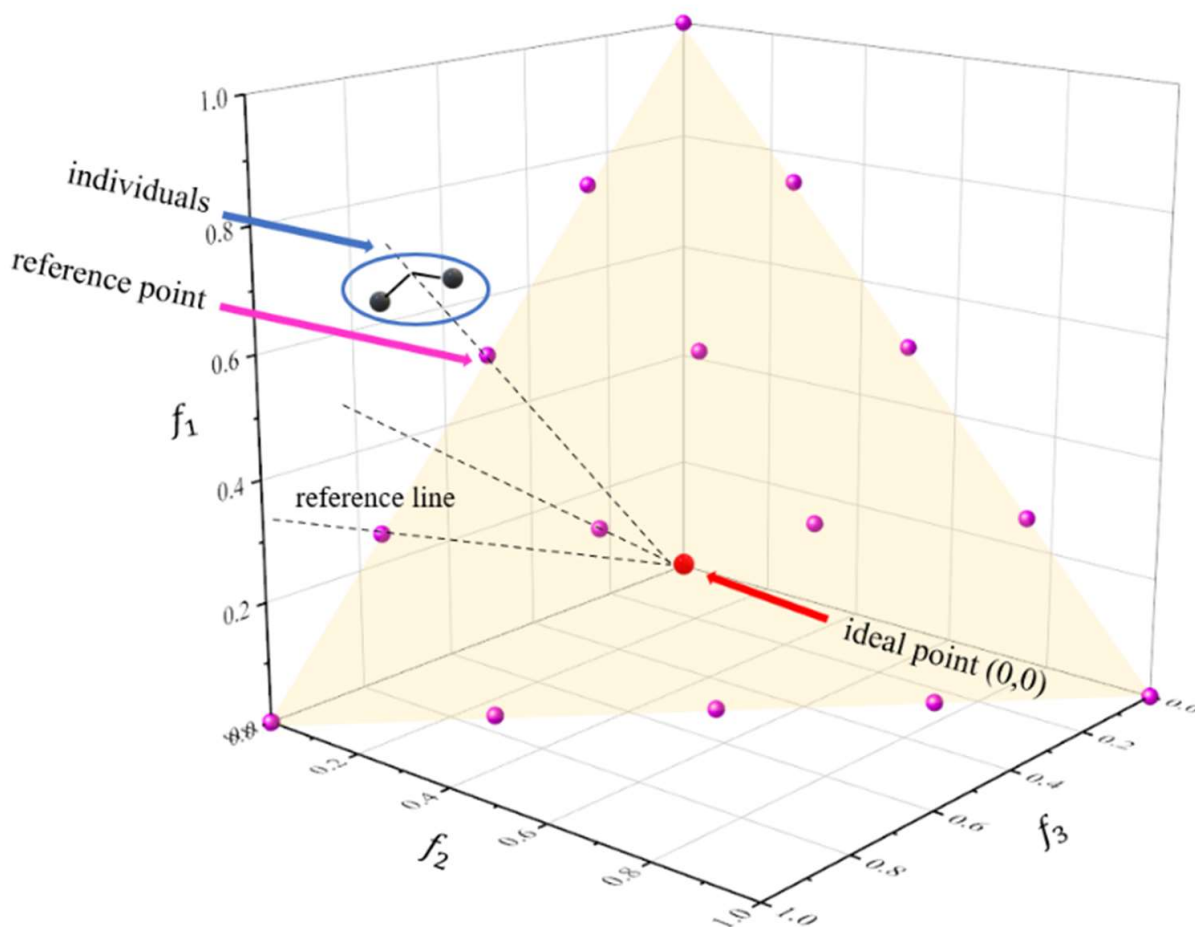


Figure 3. Association of individuals with reference points.

2.3. MOEA/D

The core principle of the MOEA/D algorithm is to decompose a multi-objective optimization problem into a set of single-objective sub-problems or multiple multi-objective

sub-problems, which finds an approximation to the entire Pareto surface (pink line in Figure 4) by using the neighbor relationships between the sub-problems to optimize all the sub-problems simultaneously in a collaborative manner [27]. Typically, the sub-problems are defined by weight vectors (black dashes in Figure 4), and the neighbor among sub-problems is determined by calculating the Euclidean distance between the weight vectors. Sum functions which are commonly applied are the weighted sum approach [31], Tchebycheff approach [32], and the penalty-based boundary intersection approach [27]. The MOEA/D algorithm used in this work is based on the implementation of the Tchebycheff approach. The result of the Tchebycheff sum function g^{tch} is calculated as:

$$g^{tch}(x | w) = \max_{i \in \{1, \dots, m\}} w_i |f_i(x) - z_i| \tag{1}$$

where i is individual; z_i is the value of the reference point z , x is the decision vector, w is the weight vector.

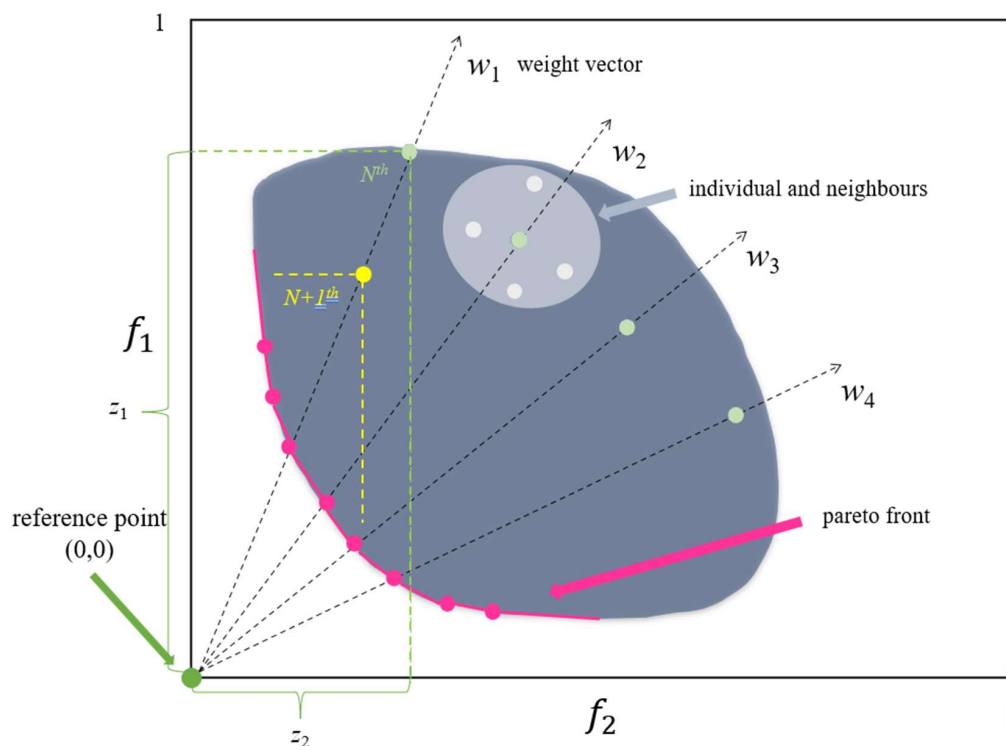


Figure 4. The procedure of MOEA/D.

2.4. Differential Evolution with NSGA-II, NSGA-III, and MOEA/D

The differential evolution (DE) algorithm is based on population differences, which finds solutions to optimization problems through cooperation and competition between individuals [33,34]. The concept of differential evolution is as follows:

Firstly, two individuals (x_{r1}, x_{r2}) are randomly selected from the population, and the difference between the individuals is multiplied by the differential weight (F), and they are added to the third individual (x_{r3}) to generate a mutant individual (v_i):

$$v_i = x_{r3} + F(x_{r1} - x_{r2}) \tag{2}$$

where v_i is mutant individual, x_{r1}, x_{r2} , and x_{r3} are selected individuals, F is differential weight.

Secondly, the mutant individual will replace the original individual in the population with a certain probability so that a test population is created:

$$u_i = \begin{cases} v_i & \text{random}(0,1) \leq Cr \text{ or } i = i_{random} \\ x_i & \text{random}(0,1) > Cr \end{cases} \quad (3)$$

where u_i is test individual, v_i is mutant individual, x_i is original individual, Cr is crossover factor. Finally, the test population is compared with the original population and better ones are retained into the next generation.

It has been found that differential evolution strategies, when introduced into multi-objective optimization algorithms, will improve the global search capability and convergence of multi-objective optimization algorithms [35,36]. However, no one has introduced a genetic algorithm based on differential evolution to the distillation sequence synthesis problem.

3. Binary Tree Coding

For ease of representation and calculation, the following two assumptions were introduced into the design of distillation sequences: (1) All components in the flow unit were arranged in ascending order according to their boiling points. (2) Each unit consists of a simple tower, and the splitting of the material is clearly split, i.e., the distillation column had only one inlet flow unit and two outlet flow units at the top and bottom of the tower, and both of them were capable of separating the light and heavy key components.

For a mixture of four components A, B, C, and D, the distillation separation sequence can be expressed in the form of ABC|D, with “|” representing the separation task, i.e., the separation of ABCD into two mixtures ABC and D, as shown in Figure 5.

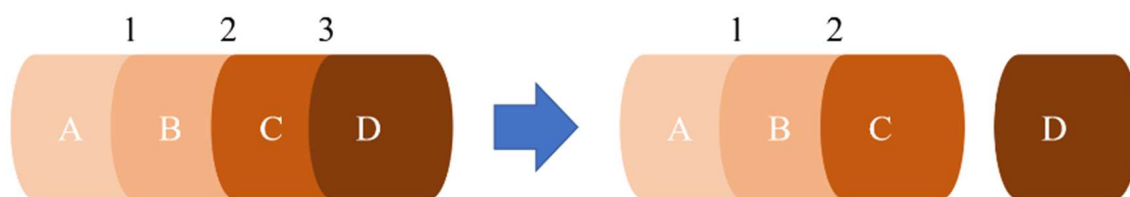


Figure 5. Separation number of four components.

In order to make the distillation sequence correspond to the array of separation tasks, the distillation sequence was encoded in a binary tree, taking into account the similarity between the structure of a sharp distillation sequence and a binary tree. For example, S [3, 1, 2] is a random task array for a distillation sequence. The three data were ordered into the binary tree, as shown in Figure 6. The child nodes were found through the pre-order traversal, and the parent nodes were found through the post-order traversal. As a result, the number of the downstream distillation columns and upstream distillation columns are determined, respectively. The ordered binary tree was S [3, 1, 2] for the pre-traversal and S [2, 1, 3] for the post-traversal.

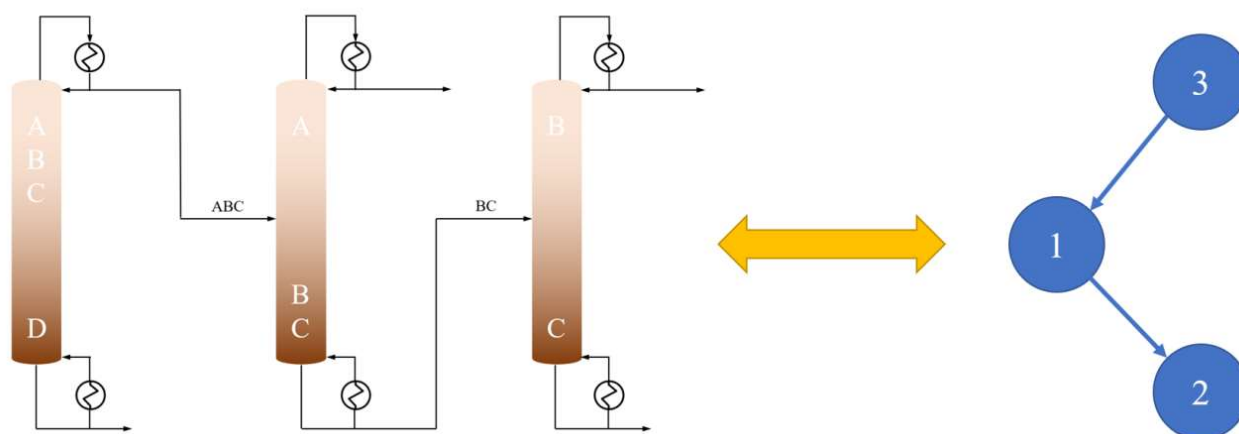


Figure 6. Diagram of separation sequence and binary tree. A, B, C, D are the four components of the mixture and 1, 2, 3 represent the numbers of separation positions.

4. Comparative Study of Evolutionary Algorithms

Due to sufficient thermodynamic data for saturated alkanes, this section illustrates the distillation separation of a 14-component alkane mixture, where a separation sequence needs to be designed to separate the components thoroughly. There are 742,900 possible combinations in a 14-component distillation sequence problem, which is complex enough to test the performance of six evolutionary algorithms. The component numbers, ingredients, molar feeds, boiling points, and K-values are listed in Table 1.

Table 1. Properties of the fourteen-component mixture.

Component ID	Component	Molar Feeds (kmol/h)	K-Values	Boiling Points (°C)
A	methane	230	256.99	−161.49
B	ethane	100	93.25	−88.60
C	propane	40	45.63	−42.04
D	<i>n</i> -butane	50	22.37	−0.50
E	<i>n</i> -pentane	130	11.34	36.07
F	<i>n</i> -hexane	100	5.86	68.73
G	<i>n</i> -heptane	110	3.08	98.43
H	<i>n</i> -octane	180	1.61	125.68
I	<i>n</i> -nonane	120	0.86	150.82
J	<i>n</i> -decane	30	0.46	174.16
K	<i>n</i> -undecane	150	0.26	195.93
L	<i>n</i> -dodecane	190	0.14	216.32
M	<i>n</i> -tridecane	90	0.07	235.47
N	<i>n</i> -tetradecane	140	0.04	253.58

The evaluation metrics of the independent separation units are expressed in terms of annual cost correlations. The optimal synthesis using rigorous simulation analysis is so complex that an evaluation function is usually specified to evaluate the designed sequence for simplicity in the design of the distillation sequence [37]. The evaluation functions are usually relative cost function [38], separation ease coefficient [39], and separation difficulty coefficient [40]. Shi and Wang [38] compared the separation coefficient and the relative cost function, concluding that the relative cost function method is more reasonable as an evaluation index. In order to test the performance of the evolutionary algorithms, relative cost function and separation difficulty coefficient were adopted as the objective functions in this work.

The relative cost function (F) is expressed as

$$F = \sum_i F_i, F_i = \left\{ (1 - f_{unc})^{2.73} + 2.41 \right\} \Delta T_b^{-0.31}, f_{unc} = \begin{cases} t/w & t \leq w \\ w/t & t > w \end{cases} \quad (4)$$

where ΔT_b is the boiling point difference between the light and heavy key components, t is the distillate rate, w is the bottom rate.

The separation difficulty coefficient (C_{DS}) is expressed as

$$C_{DS} = \frac{\lg \left[\left(\frac{x_{lk}}{x_{hk}} \right)_D / \left(\frac{x_{lk}}{x_{hk}} \right)_W \right]}{\lg \alpha_{lk,hk}} \cdot \frac{t}{t+w} \cdot \left\{ 1 + \left| \frac{t-w}{t+w} \right| \right\} \quad (5)$$

where $\left(\frac{x_{lk}}{x_{hk}} \right)_D$ is the mole fraction ratio of light and heavy key components in distillate product, $\left(\frac{x_{lk}}{x_{hk}} \right)_W$ is the mole fraction ratio of light and heavy key components in bottom product, $\alpha_{lk,hk}$ is the relative volatility of light and heavy key components, t is the distillate rate, kmol/h, w is the bottom rate, kmol/h.

The parameters used in the evolutionary algorithms are listed in Table 2. The optimization procedure was carried out on a 64-bit desktop computer with an Intel Core i7-12700 CPU @2.10 GHz, including a 16 GB RAM. Considering that multi-objective optimization algorithms are characterized by random evolution, the performance of algorithms may not be indicated by the results of a single calculation. Therefore, the calculation was repeated 100 times in this paper, and the results were statistically analyzed to find out the pattern and characteristics.

Table 2. The parameters of six evolution algorithms.

Evolution Algorithm	Parameters
NSGA-II	$dim = 2; size = 100; gen = 100; cf = 1; mf = 1/dim$
NSGA-III	$dim = 2; size = 100; gen = 100; cf = 1; mf = 1/dim$
MOEA/D	$dim = 2; size = 100; gen = 100; cf = 1; mf = 1/dim; ps = 0.9; sn = size/10$
NSGA-II-DE	$dim = 2; size = 100; gen = 100; f = 0.5; Cr = 0.5 mf = 1/dim; ps = 0.9$
NSGA-III-DE	$dim = 2; size = 100; gen = 100; f = 0.5; Cr = 0.5 mf = 1/dim; ps = 0.9$
MOEA/D-DE	$dim = 2; size = 100; gen = 100; f = 0.5; Cr = 0.5 mf = 1/dim; sn = size/10$

Where dim is dimension of the objective function, $size$ is size of population, gen is generation, cf is crossover factor, mf is mutation factor, ps is probability of selection, sn is size of neighbor, f is scaling factor in differential evolution operator.

The evaluation of the multi-objective evolutionary algorithm (MOEA) takes into account two main indicators: effectiveness and efficiency. The effectiveness refers to the quality of the Pareto optimal solution set it finds, mainly in terms of the convergence and distribution effect of MOEA. The efficiency refers to the CPU time it takes to find the Pareto solution set for a multi-objective optimization problem, and the RAM it occupies. The comprehensive evaluation metric reflects both convergence and distribution of MOEA through a scalar value. In recent years, hypervolume (HV) [41] and indicator generational distance (IGD) [42] have been widely used, and both of them are applied in evaluating the effectiveness of evolutionary algorithms.

Figure 7 shows the change in HV with the evolution of the population. The Blue dashed line represents the mean HV values of six MOEAs in each generation. The blue-filled part indicates the fluctuation of the result, which was calculated from $\mu \pm \sigma$, where μ is mean HV and σ is standard deviation. The HV value was strictly subject to the Pareto dominant principle. For example, if individual A dominates individual B, the HV value of individual A must be greater than that of individual B. As the differential evolution strategy enhanced the search ability of evolutionary algorithm, the performance of the three evolutionary algorithms was improved. At the same time, the HV value of NSGA-II-DE

was significantly higher than the others, which means NSGA-II-DE is optimal in terms of the analysis results of the HV indicator.

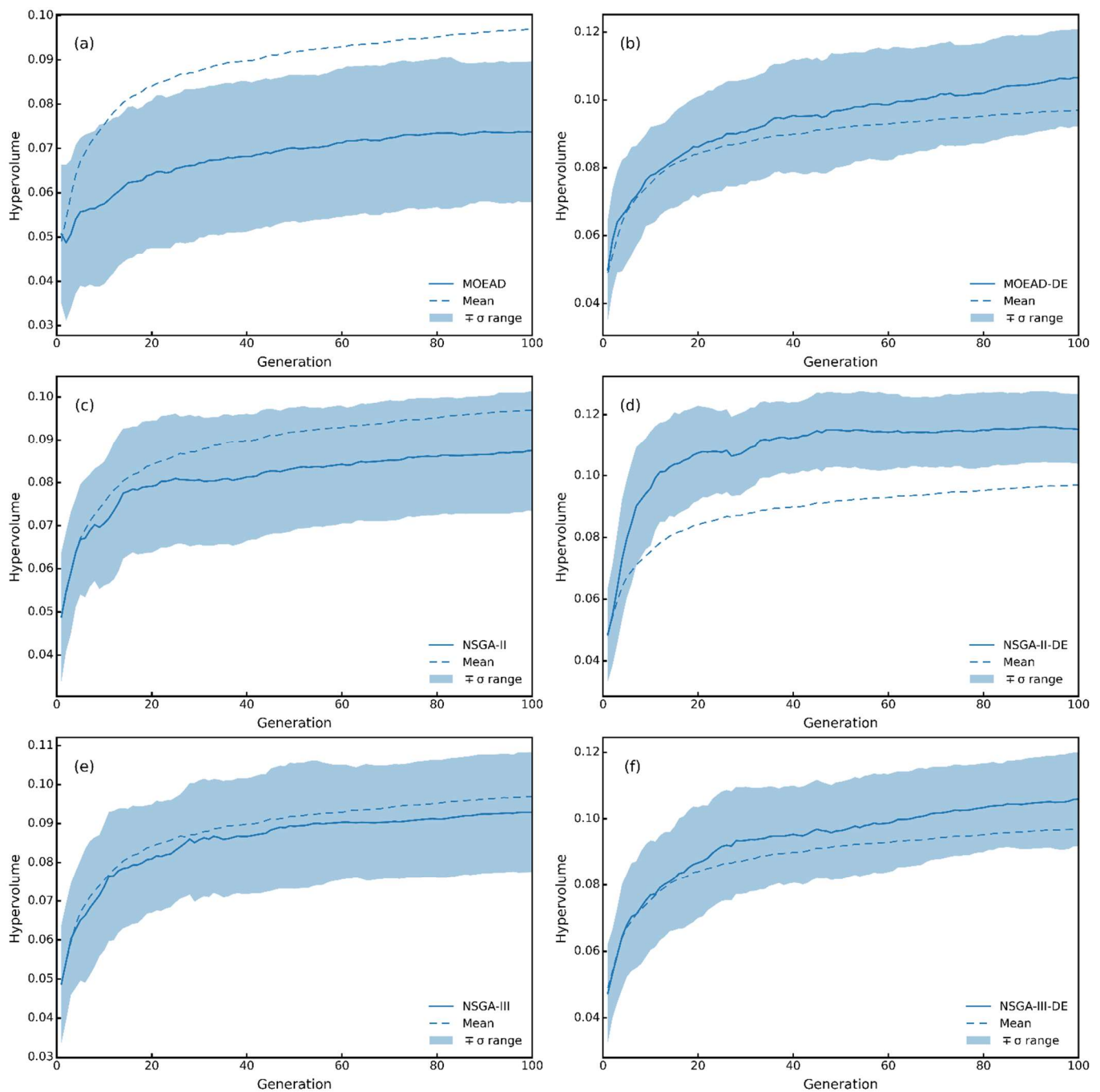


Figure 7. Hypervolume. (a) MOEAD; (b) MOEAD-DE; (c) NSGA-II; (d) NSGA-II-DE; (e) NSGA-III; (f) NSGA-III-DE.

Figure 8 shows the change in IGD with the evolution of the population. The IGD value indicates the average distance from the individuals in the Pareto set to the non-dominated solution set found by the evolutionary algorithm, which means that the smaller the value of IGD, the better the performance of the algorithm. Since the IGD value is related to the preset Pareto front curve and the Pareto front curve cannot be directly derived, an approximation was used instead of the Pareto front curve, which may have affected the

IGD values of the six algorithms. Thus, the performance of the four algorithms, except for the NSGA-II-DE and MEOA/D, was considered to be comparable.

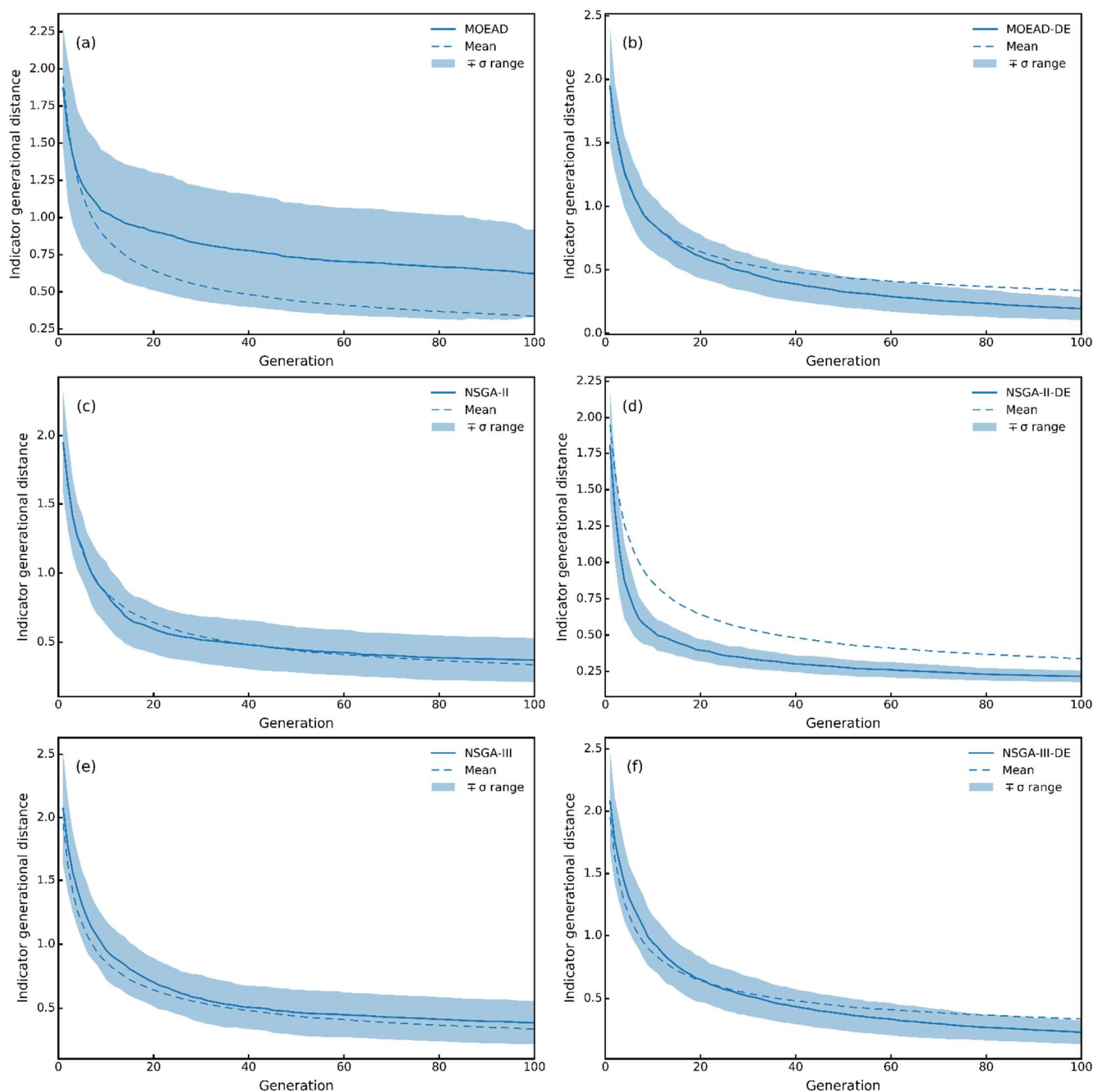


Figure 8. Indicator generational distance. (a) MOEAD; (b) MOEAD-DE; (c) NSGA-II; (d) NSGA-II-DE; (e) NSGA-III; (f) NSGA-III-DE.

From Figure 9, the size of the marker indicates the probability of recurrence 100 times. If more individuals converge to the same point, the larger the marker will be, which means a higher performance level of the algorithm. It can be seen that the non-dominated front calculated by NSGA-II-DE outperformed the non-dominated front obtained by the other algorithms, which led to the conclusion that the NSGA-II-DE algorithm performs better than the other algorithms. The convergence and distribution of NSGA-II, NSGA-III, and MEOA/D were improved by introducing the differential evolution operator as an evolutionary strategy, which is consistent with the findings reported in the literature [35,36].

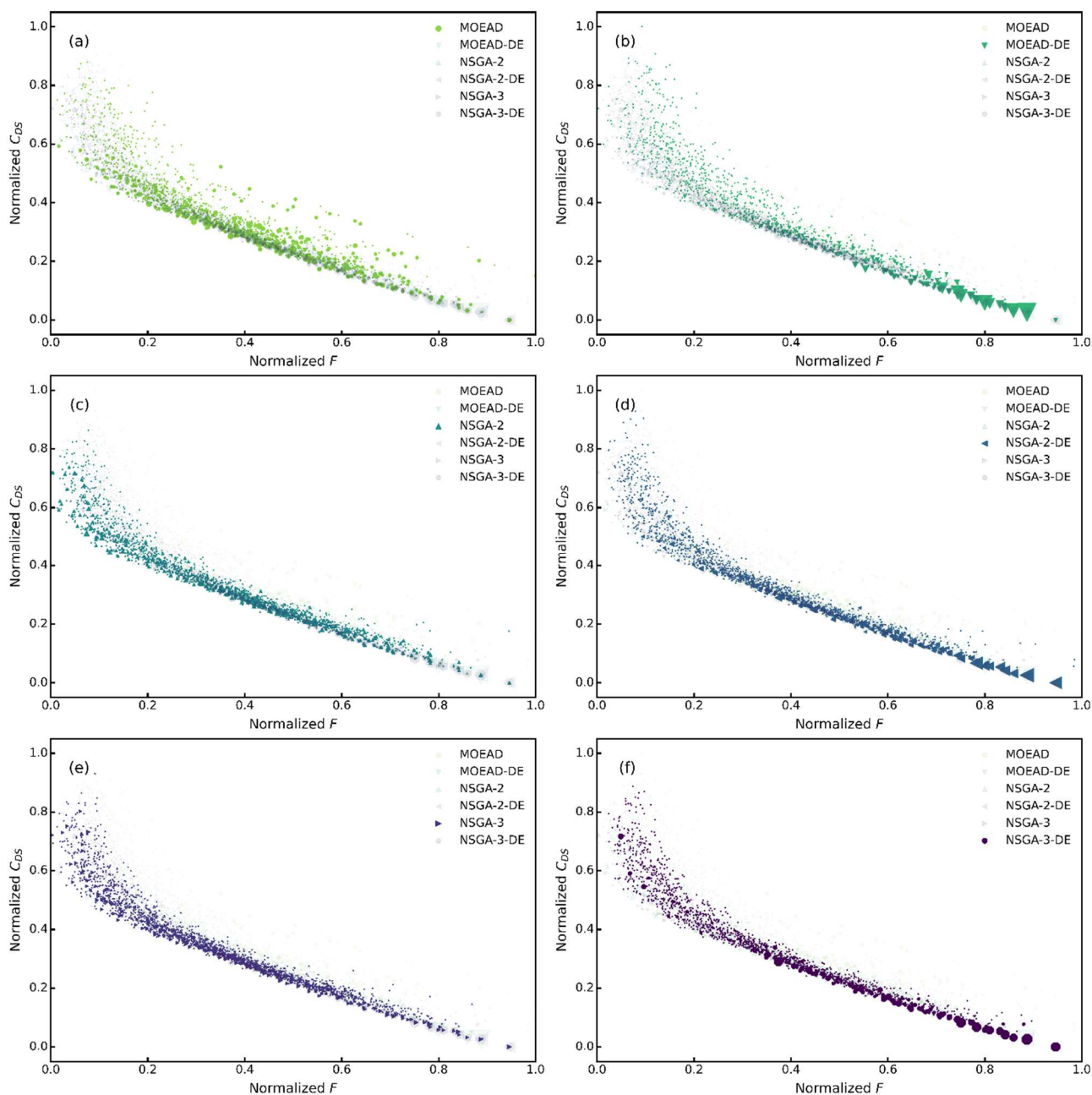


Figure 9. Non-dominated fronts. (a) MOEAD; (b) MOEAD-DE; (c) NSGA-II; (d) NSGA-II-DE; (e) NSGA-III; (f) NSGA-III-DE.

5. Optimization of the Base Case

5.1. Separation Flowsheet and Thermodynamic Modeling

This present study introduced a separation scheme proposed by Mayevskiy et al. [29] instead of redesigning a distillation sequence to separate the 6-composition mixture. The same as the reference publication, a feed flow of 100 kmol/h with molar compositions of 0.4934, 0.1717, 0.0847, 0.1927, 0.0015, and 0.0575 for acetone, isopropanol, water, methyl isobutyl ketone (MIBK), methyl isobutyl carbinol (MIBC), and diisobutyl ketone (DIBK), respectively was used.

The first column plays a role in pretreatment. The high-boiling-point components (MIBK, MIBC, DIBK) and low-boiling-point components (acetone, isopropanol, water) were divided from this column. The products of distillate and bottoms were refined in the second and third columns. A pump conveyed the stream, and the pump discharge

pressure was set at 320 kPa. The last two distillation columns were operated under negative pressure. However, because the ratio C_P/C_V for MIBK, MIBC, and DIBK (1.048, 1.045, 1.033) is relatively small, this may lead to higher operating costs for the vacuum pump. Thus, the operative pressure of the distillation column will be redesigned. The distillation sequence to be optimized is shown in Figure 10. More details can be found in Mayevskiy et al. [29].

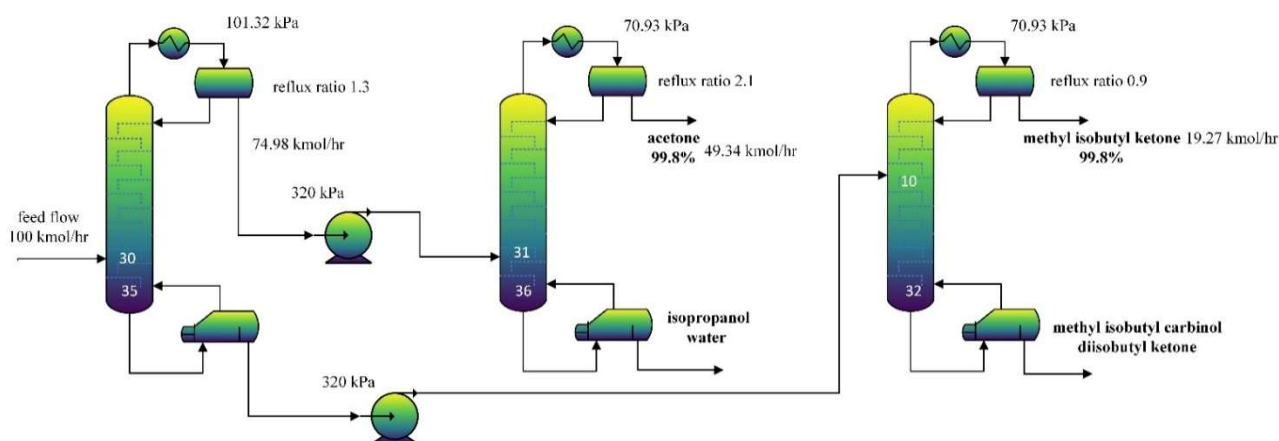


Figure 10. Flowsheet of 6-component mixture separation.

The above process was simulated by Aspen Plus v11. Design specifications were set in the RadFrac block to ensure that the product purity met the separation requirements. In the pretreatment column, molar recoveries of isopropanol in distillate and MIBK in the bottom were both 0.9995. The others were set molar purity of key components as design specifications.

To be consistent with the simulation approach in the publication, Non-Random Two-Liquid (NRTL) was chosen as the thermodynamic model. The validity of the NRTL model has been discussed in the literature [29]. However, the single activity coefficient model is not able to calculate the thermodynamic state of the gas. When it occurs, the Aspen Plus simulator uses ideal gas law to calculate the gas thermodynamic state, which compensates for this deficiency, but it can introduce theoretical errors. NRTL parameters for binary systems are shown in Table 3.

Table 3. NRTL parameters for binary systems.

Component i	Component j	A_{ij}	A_{ji}	B_{ij}	B_{ji}
Acetone	Isopropanol	−2.4106	2.4494	822.4892	−583.3452
Acetone	Water	6.3981	0.0544	−1808.9910	419.9716
Isopropanol	Water	−1.3115	6.8284	426.3978	−1483.4573
Acetone	MIBK	−5.4452	5.3013	1833.5227	−1735.9082
Isopropanol	MIBK	0.0000	0.0000	160.6435	28.1164
Water	MIBK	9.1629	−3.2305	−1248.7440	1208.8770
Water	MIBC	10.2983	−3.2359	−1367.8159	998.0640
Water	DIBK	11.6082	−0.3283	−969.9380	730.5226
MIBK	MIBC	0.3818	−0.1565	0.0000	0.0000
Acetone	MIBC	0	0	222.1975	7.9431
Acetone	DIBK	0	0	335.0488	−164.9281
Isopropanol	MIBC	0	0	159.3051	−122.9533
Isopropanol	DIBK	0	0	263.2273	125.6002
MIBK	DIBK	0	0	123.9190	−77.4980
MIBC	DIBK	0	0	89.2102	172.8563

5.2. Performance Indicators

In order to evaluate the performance of the distillation sequence, total annual cost and CO₂ emissions were adopted as indicators in this work [43,44]. The total annual cost is a

commonly used economic indicator which includes capital investments and operating costs. In the present work, the capital investments consisted of column vessel cost, column tray cost, vacuum pump cost, heat exchanger cost, and feed pump cost. Electricity consumption, cooling water consumption, and steam consumption influence operating costs.

The total annual cost is calculated as

$$\text{TAC} = \frac{\text{capital investments}}{\text{payback period}} + \text{operating cost} \quad (6)$$

where the payback period is 3 years.

The column cost is calculated as

$$C_c = \frac{MS}{280} \times 101.9 \times D_c^{1.066} \times L_c^{0.802} \times (2.18 + 3.67) \quad (7)$$

where D_c is the diameter of the column (ft); L_c is the height of the column; MS is the Marshall & Swift index. Here, M&S was taken as 1448.3. The height of the column is calculated as

$$L_c = 2.3 \times (N_T - 1) \quad (8)$$

where L_c is height of column, [ft]; N_T is the total number of trays in the column.

The tray cost is calculated as

$$C_T = \frac{MS}{280} \times 4.7 \times D_c^{1.55} \times L_c \times (1 + 1.8 + 1.7) \quad (9)$$

The cost of heat exchanger is calculated as

$$C_{he} = \frac{MS}{280} \times 5109.49 \times A^{0.65} \times (2.29 + F_c) \quad (10)$$

where A is the area of heat exchanger (ft²); F_c is 5.0625 for the reboiler and 3.75 for the condenser. For the reboiler and condenser,

$$A_R = \frac{Q_R}{U_R \Delta T_R} \quad (11)$$

$$A_C = \frac{Q_C}{U_C \Delta T_C} \quad (12)$$

where A_R and A_C is heat transport area of reboiler and condenser, respectively (m²); U_R is the transfer coefficient for re boiler (kW/(K·m²)), ΔT_R is the temperature difference, (K). U_c is the transfer coefficient for condenser (kW/(K·m²)), ΔT_c is the temperature difference (K). Here, U_R was taken as 0.568 and U_c was taken as 0.852.

The cost of vacuum pump and feed pump are given as [45]

$$C_{vp} = 4200 \times \left(\frac{60 \times F_v \times 8.314 \times 273.15}{3600 \times 101325} \right)^{0.55} \quad (13)$$

where F_v is the volumetric flow rate (kmol/h).

$$C_{fp} = 26700 \times \left(\frac{24 \times F_f \times 3600}{50000} \right)^{0.53} \quad (14)$$

where F_f is the feed flow rate (m³/s).

The utility cost is calculated as

$$C_{LP} = 7.07 \times Q_{LP} \times 8000 \quad (15)$$

$$C_{MP} = 8.57 \times Q_{MP} \times 8000 \quad (16)$$

$$C_{CW} = 0.354 \times Q_{CW} \times 8000 \tag{17}$$

$$C_E = 0.0775 \times Q_E \times 8000 \tag{18}$$

where C_{LP} is the cost of lower pressure steam (3 bar); Q_{LP} is the lower pressure steam duty (GJ); C_{MP} is the cost of medium pressure steam (15 bar); Q_{MP} is the medium pressure steam duty (GJ); C_{CW} is the cost of cooling water (298.15 K); Q_{CW} is the cooling water duty (GJ); C_E is the cost of electricity; Q_E is the electricity duty (kW).

In considering the impact of distillation separation on the environment, this work used Greenhouse gas emissions as an evaluation index. This methodology was proposed by Gadalla et al. [46] and CO₂ emissions can be calculated with the following equation.

$$\text{CO}_2 \text{ emissions} = \left(\frac{Q_{Fuel}}{NHV} \right) \left(\frac{C\%}{100} \right) a \tag{19}$$

where Q_{Fuel} is amount of fuel burnt (kW); a is the ratio of molar masses of CO₂ and C; NHV represents the net heating value of fuel with a carbon content of C% (kJ/kg).

5.3. Optimization Methodology and Objective Function

The improved non-dominated sorting genetic algorithm II based on differential evolution algorithm (NSGA-II-DE) was applied to optimize the distillation sequence to provide quantitative benefits and trade-offs between annual operating costs and capital investments. The NSGA-II-DE procedure includes initiation of population, evolution, and end, as shown in Figure 11. The optimization of the distillation sequence is based on the Aspen Plus v11, which enables communication between python and Aspen Plus through ActiveX [47]. The design parameters were generated by a Python program and entered into Aspen Plus simulator via the COM technique. After the simulation was completed without errors, the Aspen Plus simulator returned the results (TAC and CO₂ emissions) to Python. TAC and CO₂ emissions were calculated using the calculator module of Aspen Plus. The NSGA-II-DE was used in Python to analyze the corresponding objective functions under different design parameters, evolving until the number of generations satisfied 100 generations.

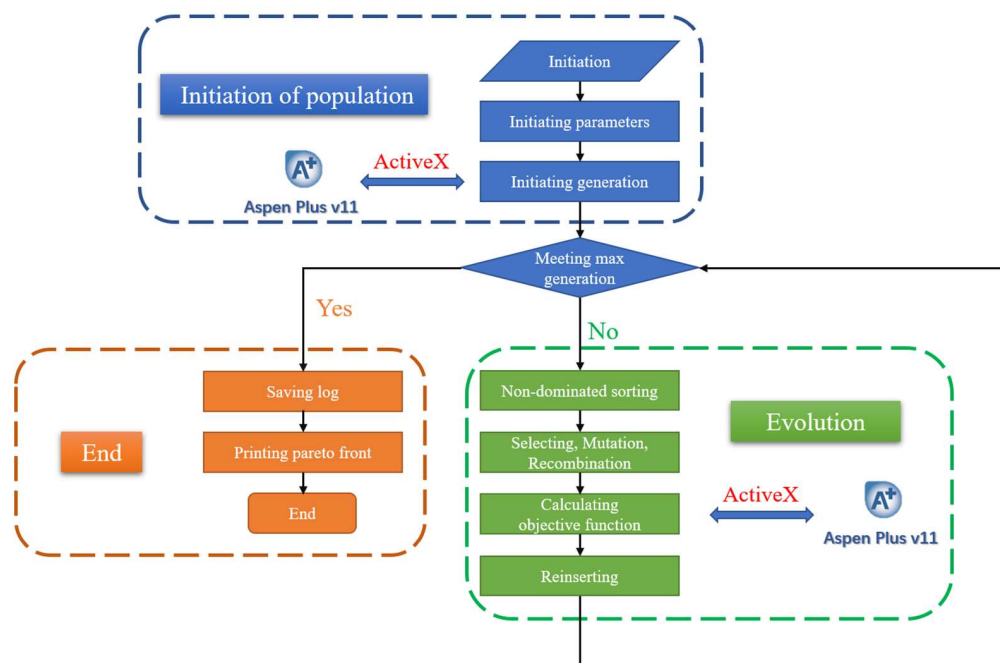


Figure 11. Aspen Plus calculations with NSGA-II-DE for the distillation sequence.

The two targets mentioned already were accounted for in the objective function, which is defined as follow:

$$\min(\text{TAC}, \text{CO}_2) = f(N_T, N_F, R, F_d, P) \quad (20)$$

where TAC is total annual cost (million\$); CO_2 is CO_2 emissions (kt/year); N_t is the total number of trays in the column; N_F is feed stage, R is mole reflux ratio, F_d is distillate rate (kmol/h); P is operative pressure (kPa). The objective function is restricted by fulfilling the molar purity of the key component upper than 0.998 or molar recovery of the key component upper than 0.999.

In this example, the feed plate was changed to the ratio of the feed plate to the number of plates, and the result was rounded down to ensure that the feed plate is always smaller than the total number of plates. The total number of design variables, in this case, was 15. To ensure that the molar purity of the product reached 99.8%, the design specifications were set in the RadFrac block. At the same time, the molar recoveries of the key components are charged at 99.9%. There are still nine design variables, which can be found in Table 4.

Table 4. Range of variation in population individual.

Decision Variable	Variable Category	Change Range
T1 total number of trays	integer	[30,60]
T1 ratio of the feed stage to the total number of trays	real number	[0.1,0.95]
T1 operative pressure	integer	[40,100]
T2 total number of trays	integer	[30,60]
T2 ratio of the feed stage to the total number of trays	real number	[0.1,0.95]
T2 operative pressure	integer	[40,85]
T3 total number of trays	integer	[30,60]
T3 ratio of the feed stage to the total number of trays	real number	[0.1,0.95]
T3 operative pressure	integer	[60,100]

5.4. Optimization Results

In this work, the optimization procedure was carried out on a 64-bit desktop computer with an Intel Core i7-12700 CPU @2.10 GHz, including 16 GB RAM. The parameters of NSGA-II-DE are the same as the ones listed in Table 2. The program took about 8 h to obtain the optimization results. The non-dominated front is shown in Figure 12.

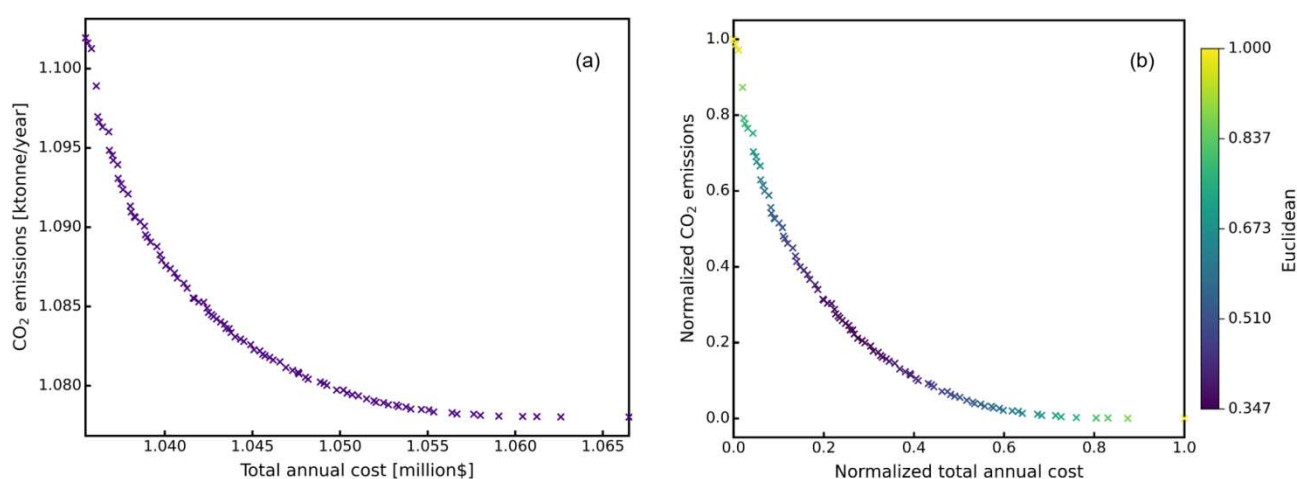


Figure 12. Pareto sets of TAC and CO_2 emissions: (a) raw result and (b) normalized result.

By increasing the number of plates, the separation performance of the distillation column can be improved, and therefore the equipment investment also increases. When the number of plates was increased or decreased to a certain level, there was no significant reduction in CO_2 emission or total annual cost. At the same time, the total annual cost and

CO₂ emissions were normalized, which makes it possible to directly find the Euclidean distance from the ideal point (0,0) for the results to compare the superiority of the individuals on the non-dominated front. In Figure 12b, the darker the scatter color, the closer to the ideal point.

The optimization results are shown in Table 5. By optimizing the operational parameters of the distillation sequence through NSGA-II-DE, the total annual cost was reduced by 1.868 million\$, and CO₂ emission was reduced by 5.002 kt/year. The CO₂ emission and total annual cost were reduced by 64.15% and 82.23%. As expected, a reduced-pressure distillation operation in the T3 column would incur significant energy costs, making it more suitable for atmospheric pressure separation.

Table 5. Comparison between initial results and NSGA-II-DE optimization results.

Operation Parameters	Base Case [29]	After Optimization (Min Euclidean Distance)
T1 total number of trays	35	56
T1 feed stage	30	47
T1 operative pressure (kPa)	101.32	100
T2 total number of trays	36	43
T2 feed stage	31	37
T2 operative pressure (kPa)	70.93	58
T3 total number of trays	32	58
T3 feed stage	10	23
T3 operative pressure (kPa)	70.93	100
TAC (million\$)	2.912	1.044
CO ₂ Emission (kt/year)	6.083	1.083

6. Conclusions

This work presented the performance test of six evolutionary algorithms used in previous work. Firstly, the 14-component distillation sequence problem was successfully solved. The Pareto charts of each algorithm showed that the algorithms with differential evolution would improve their global search capability and convergence, and NSGA-II-DE performed the best. Secondly, a triple-column distillation sequence in the publication was optimized by using NSGA-II-DE. By optimizing the feed stage, the number of trays, and operative pressure, the CO₂ emission and total annual cost were reduced by 64.15% and 82.23%, respectively. This study demonstrated the ability of NSGA-II-DE to obtain the optimal synthesis of the distillation sequence and explores an overall solution of distillation separation design.

Author Contributions: Conceptualization, Z.H. and Y.L.; methodology, Z.H.; software, Z.H.; validation, Z.H.; investigation, P.L.; resources, Y.L.; data curation, P.L.; writing—original draft preparation, Z.H.; writing—review and editing, Y.L., Z.H.; visualization, Z.H.; supervision, Y.L.; project administration, Y.L.; funding acquisition, Y.L. All authors have read and agreed to the published version of the manuscript.

Funding: This research was funded by Natural Science Foundation of Jiangsu Province, grant number BK20160978.

Institutional Review Board Statement: Not applicable.

Informed Consent Statement: Not applicable.

Data Availability Statement: The data presented in this study are available on request from the corresponding author.

Conflicts of Interest: The authors declare no conflict of interest.

Sample Availability: Samples of the compounds are not available from the authors.

References

1. Lockhart, F.J. Multi-column distillation of natural gasoline. *Pet. Refin.* **2016**, *26*, 104.
2. Siirola, J.J.; Powers, G.J.; Rudd, D.F. Synthesis of system designs: III. Toward a process concept generator. *AIChE J.* **1971**, *17*, 677–682. [[CrossRef](#)]
3. Gao, X.C.; Li, Z.; Chen, C.; Da, C.; Liu, L.; Tian, S.; Ji, G.C. The determination of pore shape and interfacial barrier of entry for light gases transport in amorphous teos-derived silica: A finite element method. *ACS Appl. Mater. Interfaces* **2021**, *13*, 4804–4812. [[CrossRef](#)] [[PubMed](#)]
4. Gao, X.C.; Da, C.; Chen, C.; Li, Z.H.; Gu, X.H.; Bhatia, S.K. The induced orientation effect of linear gases during transport in a NaA zeolite membrane modified by alkali lignin. *J. Membr. Sci.* **2021**, *620*, 118971. [[CrossRef](#)]
5. Wang, J.C.; Zhang, J.Q.; Hong, Z.; Gao, X.C.; Gu, X.H. A coupling process of distillation with vapor permeation and adsorption for production of fuel ethanol: A comparative analysis on energy consumption. *Ind. Eng. Chem. Res.* **2022**, *61*, 1167–1178. [[CrossRef](#)]
6. Gao, X.C.; Wang, S.H.; Wang, J.C.; Xu, S.F.; Gu, X.H. The study on the coupled process of column distillation and vapor permeation by NaA zeolite membrane for ethanol dehydration. *Chem. Eng. Res. Des.* **2019**, *150*, 246–253. [[CrossRef](#)]
7. Han, W.T.; Han, Z.W.; Gao, X.C.; Hong, Z.; Li, X.G.; Li, H.; Gu, X.H.; Gao, X. Inter-integration reactive distillation with vapor permeation for ethyl levulinate production: Equipment development and experimental validating. *AIChE J.* **2022**, *68*, e17441. [[CrossRef](#)]
8. Heaven, L.D. *Optimum Sequencing of Distillation Columns in Multicomponent Fractionation*; University of California: Berkeley, CA, USA, 1969.
9. Thompson, R.W.; King, C.J. Systematic synthesis of separation schemes. *AIChE J.* **1972**, *18*, 941–948. [[CrossRef](#)]
10. Freshwater, D.C.; Henry, B.D. Optimal configuration of multicomponent distillation systems. *Chem. Eng.* **1975**, *9*, 533–540.
11. Seader, J.D.; Westerberg, A.W. A combined heuristic and evolutionary strategy for synthesis of simple separation sequences. *AIChE J.* **1977**, *23*, 951–954. [[CrossRef](#)]
12. Tayal, M.C.; Fu, Y.; Diwekar, U.M. Optimal design of heat exchangers: A genetic algorithm framework. *Ind. Eng. Chem. Res.* **1999**, *38*, 456–467. [[CrossRef](#)]
13. Aggarwal, A.; Floudas, C.A. Synthesis of general distillation sequences-nonsharp separations. *Comput. Chem. Eng.* **1990**, *14*, 631–653. [[CrossRef](#)]
14. Floquet, P.; Pibouleau, L.; Domenech, S. Separation sequence synthesis: How to use simulated annealing procedure? *Comput. Chem. Eng.* **1994**, *18*, 1141–1148. [[CrossRef](#)]
15. Leboireiro, J.; Acevedo, J. Processes synthesis and design of distillation sequences using modular simulators: A genetic algorithm framework. *Comput. Chem. Eng.* **2004**, *28*, 1223–1236. [[CrossRef](#)]
16. Errico, M.; Pirellas, P.; Torres-Ortega, C.E.; Rong, B.G.; Segovia-Hernandez, J.G. A combined method for the design and optimization of intensified distillation systems. *Chem. Eng. Process. Process Intensif.* **2014**, *85*, 69–76. [[CrossRef](#)]
17. Vázquez-Castillo, J.A.; Segovia-Hernández, J.G.; Ponce-Ortega, J.M. Multiobjective optimization approach for integrating design and control in multicomponent distillation sequences. *Ind. Eng. Chem. Res.* **2015**, *54*, 12320–12330. [[CrossRef](#)]
18. Contreras-Zarazúa, G.; Vázquez-Castillo, J.A.; Ramírez-Márquez, C.; Segovia-Hernández, J.G.; Alcántara-Ávila, J.R. Multi-objective optimization involving cost and control properties in reactive distillation processes to produce diphenyl carbonate. *Comput. Chem. Eng.* **2017**, *105*, 185–196. [[CrossRef](#)]
19. Cabrera-Ruiz, J.; Santaella, M.A.; Alcántara-Ávila, J.R.; Segovia-Hernández, J.G.; Hernández, S. Open-loop based controllability criterion applied to stochastic global optimization for intensified distillation sequences. *Chem. Eng. Res. Des.* **2017**, *123*, 165–179. [[CrossRef](#)]
20. Alcocer-García, H.; Segovia-Hernández, J.G.; Prado-Rubio, O.A.; Sánchez-Ramírez, E.; Quiroz-Ramírez, J.J. Multi-objective optimization of intensified processes for the purification of levulinic acid involving economic and environmental objectives. *Chem. Eng. Process.* **2019**, *136*, 123–137. [[CrossRef](#)]
21. Sun, S.R.; Chun, W.; Yang, A.; Shen, W.F.; Cui, P.Z.; Ren, J.Z. The separation of ternary azeotropic mixture: Thermodynamic insight and improved multi-objective optimization. *Energy* **2020**, *206*, 118117. [[CrossRef](#)]
22. Zhang, Y.Z.; He, N.E.; Masuku, C.M.; Biegler, L.T. A multi-objective reactive distillation optimization model for Fischer-Tropsch synthesis. *Comput. Chem. Eng.* **2020**, *135*, 106754. [[CrossRef](#)]
23. Zhao, F.; Xu, Z.F.; Zhao, J.G.; Wang, J.; Hu, M.Y.; Li, X.; Zhu, Z.Y.; Cui, P.Z.; Wang, Y.L.; Ma, Y.X. Process design and multi-objective optimization for separation of ternary mixtures with double azeotropes via integrated quasi-continuous pressure-swing batch distillation. *Sep. Purif. Technol.* **2021**, *276*, 119288. [[CrossRef](#)]
24. Deb, K.; Pratap, A.; Agarwal, S.; Meyarivan, T. A fast and elitist multiobjective genetic algorithm: NSGA-II. *IEEE Trans. Evol. Comput.* **2002**, *6*, 182–197. [[CrossRef](#)]
25. Deb, K.; Jain, J. An evolutionary many-objective optimization algorithm using reference-point-based nondominated sorting approach, part I: Solving problems with box constraints. *IEEE Trans. Evol. Comput.* **2014**, *18*, 577–601. [[CrossRef](#)]
26. Tanabe, R.; Fukunaga, A. Reevaluating exponential crossover in differential evolution. In *International Conference on Parallel Problem Solving from Nature*; Springer: Cham, Switzerland, 2014.
27. Zhang, Q.; Li, H. MOEA/D: A multiobjective evolutionary algorithm based on decomposition. *IEEE Trans. Evol. Comput.* **2007**, *11*, 712–731. [[CrossRef](#)]

28. Li, H.; Zhang, Q. Multiobjective optimization problems with complicated Pareto sets, MOEA/D and NSGA-II. *IEEE Trans. Evol. Comput.* **2009**, *13*, 284–302. [[CrossRef](#)]
29. Mayevskiy, M.; Frolkova, A.; Frolkova, A. Separation and purification of methyl isobutyl ketone from acetone + isopropanol + water + methyl isobutyl ketone + methyl isobutyl carbinol + diisobutyl ketone mixture. *ACS Omega* **2020**, *5*, 25365–25370. [[CrossRef](#)]
30. Srinivas, N.; Deb, K. Multiobjective optimization using nondominated sorting in genetic algorithms. *Evol. Comput.* **1994**, *2*, 221–248. [[CrossRef](#)]
31. Hillermeier, C. *Nonlinear Multiobjective Optimization*; Birkhauser Verlag: Basel, Switzerland, 2001.
32. Jaszkievicz, A. On the performance of multiple-objective genetic local search on the 0/1 knapsack problem—a comparative experiment. *IEEE Trans. Evol. Comput.* **2000**, *6*, 402–412. [[CrossRef](#)]
33. Storn, R.; Price, K. Differential evolution: A simple and efficient adaptive scheme for global optimization over continuous spaces. *ICSI Berkeley* **1995**, *11*, 341–359.
34. Storn, R.; Price, K. Differential evolution: A simple and efficient heuristic for global optimization over continuous spaces. *J. Glob. Optim.* **1997**, *11*, 341–359. [[CrossRef](#)]
35. Pan, X.Y.; Zhu, J.; Chen, H.; Chen, X.J.; Hu, K.K. A differential evolution-based hybrid NSGA-II for multi-objective optimization. In Proceedings of the 2015 IEEE 7th International Conference on Cybernetics and Intelligent Systems (CIS) and IEEE Conference on Robotics, Automation and Mechatronics (RAM), Siem Reap, Cambodia, 15–17 July 2015; pp. 81–86.
36. Angira, R.; Babu, B.V. Non-dominated sorting differential evolution (NSDE): An extension of differential evolution for multi-objective optimization. In Proceedings of the 2nd Indian International Conference on Artificial Intelligence, DBLP, Pune, India, 20–22 December 2005.
37. Malone, M.F.; Glinos, K.; Marquez, F.E.; Douglas, J.M. Simple analytical criteria for the sequencing of distillation columns. *AIChE J.* **1985**, *31*, 683–689. [[CrossRef](#)]
38. Shi, B.C.; Wang, J.H. Establishment and application of relative cost function for multicomponent separating column series. *J. Chem. Ind. Eng.* **1997**, *48*, 175–179.
39. Zou, R.J. *Petrochemical Separation Principles and Technology*; Chemical Industry Press: Beijing, China, 1983.
40. Nath, R.; Motard, L.R. Evolutionary synthesis of separation process. *AIChE J.* **1981**, *27*, 578–587. [[CrossRef](#)]
41. Zitzler, E. Evolutionary algorithms for multiobjective optimization: Methods and applications. Ph.D. Thesis, Swiss Federal Institute of Technology, Zürich, Switzerland, 1999.
42. Czyzszak, P.; Jaszkievicz, A. Pareto simulated annealing—a metaheuristic technique for multiple-objective combinatorial optimization. *J. Multi-Criteria. Decis. Anal.* **1998**, *7*, 34–47. [[CrossRef](#)]
43. Douglas, J.M. *Conceptual Design of Chemical Processes*; McGraw-Hill, Inc.: New York, NY, USA, 1998.
44. Luyben, W.L. A counter-intuitive heuristic for specifying the composition of recycle streams. *Chem. Eng. Process.* **2018**, *133*, 234–244. [[CrossRef](#)]
45. Oliveira, T.A.; Cocchini, U.; Scarpello, J.T.; Livingston, A.G. Pervaporation mass transfer with liquid flow in the transition regime. *J. Membr. Sci.* **2001**, *183*, 119–133. [[CrossRef](#)]
46. Gadalla, M.A.; Olujic, Z.; Jansens, P.J.; Jobson, M.; Smith, R. Reducing CO₂ emissions and energy consumption of heat-integrated distillation systems. *Environ. Sci. Technol.* **2005**, *39*, 6860–6870. [[CrossRef](#)]
47. Su, Y.; Jin, S.M.; Zhang, X.P.; Shen, W.F.; Eden, M.R.; Ren, J.Z. Stakeholder-oriented multi-objective process optimization based on an improved genetic algorithm. *Comput. Chem. Eng.* **2020**, *132*, 106618. [[CrossRef](#)]